Research Article

Computer Geometric Modeling and CFD Simulation of Air Permeability in Knitted Fabrics

Wasit Chaikumming[1], Theeradech Songart[1], Puttipong Patumchat[2] and Keartisak Sriprateep[1]*

[1]*Manufacturing and Materials Research Unit (MMR), Department of Manufacturing Engineering, Faculty of Engineering, Mahasarakham University, Mahasarakham, Thailand*

[2]*Department of Industrial Piping Technology, Faculty of Technical Education, Rajamangala University of Technology Isan Khonkaen Campus, Khonkaen, Thailand*

* Corresponding Author: keartisak.s@msu.ac.th

ARTICLE INFO	ABSTRACT
	The purpose of this study is to model the geometry of knitted fabric structures to predict air permeability using computational fluid dynamics (CFD). Rib 1×1 and interlock structures were simulated with varying loop densities and plain weft-knitted fabric models. The geometrical models of plain weft-knitted fabrics were studied using the Peirce model, the Leaf and Glaskin model, the Vassiliadis model, and Kurbak model, which considers the real shape of knit loops in three-dimensional space. A unit cell for each model was created with a single line of yarn path using SolidWorks software. Computational fluid dynamics analysis was then conducted on all samples using the SolidWorks Flow Simulation package. The numerical results demonstrated good agreement with the experimental data. The presented models provide a useful framework for predicting the air permeability of knitted fabrics by employing unit cells of the knitted fabric structure. This approach reduces operational complexity and significantly shortens solution time. **Keywords:** Geometric Modeling, Computer Aided Design (CAD), Computational fluid Dynamics (CFD), Knitted fabric, Air permeability, Simulation.

I. INTRODUCTION

Porosity and pore qualities, the fluid properties that flow through the fabric, and environmental conditions are the main factors that determine a fabric's ability to permit air to pass through. Yarn type, yarn diameter, and loop density are also influenced by the fabric's porosity. Consequently, the air permeability performance of a fabric can be regulated by managing the pore properties, fluid properties, and environmental factors [1]. "Effective porosity," a term introduced by Burleigh [2], is used to describe the total porosity that determines fluid flow. It can be characterized by three distinct elements: (1) intrafiber porosity, which refers to the voids within the internal walls of fibers; (2) interfiber porosity, which describes the empty spaces within the yarn created by the arrangement of fibers; and (3) interyarn porosity, which represents the voids formed between the yarns themselves. Numerous researchers have focused on predicting the air permeability of knitted and woven fabrics [3-7] based on their structural characteristics. Given the increasing interest in three-dimensional modeling, several studies have concentrated on the geometric description of knitted loops. Researchers [8-10] have each proposed distinct methods to advance this area of research.

Many researchers have developed 3D CAD models of fibers, ply yarns, and woven fabrics [11-15]. These models have also been used to predict the tensile properties of yarn structures [16-17]. In the context of air permeability in knitted fabrics, computational fluid dynamics (CFD) methods have been employed to model and simulate the air permeability of two-layer knitted fabrics at both the single-yarn and filament levels. Puszkarz and Krucinska [18] conducted experimental investigations and computer modeling, finding that the simulation results closely aligned with experimental data for air flow through fabric models. The study of thermal insulation in knitted fabrics by Puszkarz and Krucinska [19], realized through mono-fiber and multi-fiber 3D models, demonstrated that both experimental measurements and simulations produced comparable results. Similarly, Cimilli et al. [20] utilized CFD models to determine the natural convective heat transfer coefficient for plain knitted fabrics. The 3D geometry of the plain knit fabric loop was designed using CATIA software, and CFD analysis was performed using Fluent

software. Dehkordi et al. [21] applied CFD methods to simulate the air permeability of knitted fabrics with rib and interlock structures. For each sample, a unit cell with a single line of the yarn path was created using CATIA software based on the Vassiliadis model. CFD analysis was subsequently conducted on all samples using Fluent software. Two turbulence models, k-ε and k-ω, were utilized for the analysis. The study concluded that CFD modeling is an efficient method for predicting air permeability.

There are relatively few studies that have modeled plain knitted fabrics for rib or interlock structures using unit cells and computational fluid dynamics (CFD) techniques. The primary objective of this study is to design and implement 3D models of rib and interlock knitted fabrics using the Peirce model, the Leaf and Glaskin model, the Vassiliadis model, and the Kurbak model, which represents the knit loop in three-dimensional space through specialized CAD software. A geometric model of the knit loop was developed using a single-line yarn path representation. Subsequently, CFD analysis was performed on the unit cell of the knitted fabric structure to predict its air permeability. The predicted results were subsequently compared with experimental data.

II. MATERIALS AND METHODS

A. Materials

All knitted fabrics were produced using a Mayer & Cie® double-jersey circular knitting machine with cotton/polyester yarn (30-denier count, 0.22 mm diameter). Fabrics were manufactured in rib 1x1 and interlock patterns [21]. Air permeability tests were conducted using a Shirley Air Permeability Tester, following the ASTM D737-96 standard. The pressure difference between the two sides of the fabric was maintained at a constant 100 Pa. Ten measurements were taken for each sample. Table 1 summarizes the structural and physical properties of the knitted samples.

Table 1: Structural and physical parameters of knitted samples [21].

Sample code	Pattern	Wale/cm	Course/cm	Thickness (mm)	Weight (g/m²)
R1	1x1 Rib	9	11	0.56	130.82
R2	1x1 Rib	9	13	0.58	134.61
R3	1x1 Rib	9	14	0.63	151.23
I1	Interlock	9	11	0.70	278.04
I2	Interlock	11	16	0.79	246.70
I3	Interlock	11	18	0.81	264.14

B. Geometry of plain-knitted loop

Many geometrical models have been developed by researchers for plain knitted fabrics, including those by many researchers [22-26]. In addition, some researchers have modified plain knit models to represent more complex knitted fabric structures. The primary motivations for developing geometrical models include the following: (a) identifying the factors influencing dimensional changes during relaxation; (b) organizing fabric production before initiating the knitting process; (c) facilitating technical textile applications; (d) enabling computer simulations of knitted fabrics for design or flaw evaluation purposes; (e) determining the surface properties of fabrics; and (f) preparing foundational tasks for constructing actual models, among others. This study presents a detailed geometric analysis of knitted fabrics as follows:

- **Peirce's model**

Peirce [22] developed a three-dimensional model based on the premise that the central axis of the yarn forming a course lies on a circular cylindrical surface, with the cylinder's central axis following the path of the course. He further assumed that, when the cylinder is projected onto a plane, the yarn's axis in its planar form consists of circular arcs and straight lines. Using these modeling considerations, Peirce derived the following equation for calculating the loop length:

$$l = \frac{2}{c} + \frac{1}{w} + 5.94D \qquad (1)$$

where l is the length of yarn in one loop (in mm), C is the course density (courses per mm), W is the wale density (wales per mm), and D is the apparent diameter of the yarn (in mm).

- **Leaf and Glaskin's model**

Leaf and Glaskin [23] proposed that the projection of the central axis of yarn onto the plane of the fabric is composed of circular arcs. In other words, the yarn forming a course lies on the surface of a series of circular cylinders whose central axes are perpendicular to the fabric plane. Using specific assumptions, Leaf and Glaskin derived an approximation for the length of yarn in a loop. The approximate equations (Eqs. 2-4) were found to be more accurate than the initial equations, particularly for fabrics produced using cotton yarns, at least within the range of samples analyzed. The symbols C (courses per inch), W (wales per inch), D (inches), and l (inches) in the following equations correspond to the parameters described above.

$$l = 4a\varphi D \tag{2}$$

where:

$$\varphi = \pi + \sin^{-1}\left\{\frac{C^2 D}{\sqrt{C^2 + W^2(1 - C^2 D^2)^2}}\right\} - \tan^{-1}\left\{\frac{C}{W(1 - C^2 D^2)}\right\} \tag{3}$$

$$a = 1/(4WD\sin\varphi) \tag{4}$$

- **Kurbak's model**

Kurbak's model [24-25] provides a comprehensive framework for understanding the geometric and mechanical characteristics of knitted structures. This model integrates principles from engineering, mechanics, and textile science to explain how loops interact to form a cohesive fabric structure. In this model, the upper and lower parts of the loop are represented as elliptical curves, while the arms of the loop are helical in shape. These helical arms are wrapped around elliptical cylinders that are aligned parallel to the direction of the wales, with variable helix angles.

The elliptical shape representing the top of the loop is situated in a plane that forms an angle α_1 with the horizontal y-axis. This plane extends towards the fabric thickness and terminates at a point B, where the ellipse angles are $\theta = 90^{\circ}$ on both sides in the fabric width (x-direction). The major and minor radii of the elliptical cross-sections of the cylinders, which serve as the wrapping surfaces for the central axis of the loop arms, are given by $a = t_1 d/2$ and $b = e_1 d/2$, respectively. Here, a lies in the y-direction (the thickness direction), b lies in the x-direction (the course direction), t_1 represents the diameter of the yarn arm cylinder along the thickness direction, e_1 represents the diameter along the course direction, and d denotes the effective yarn diameter.

As an assumption, the equation of the curve between the points on the right arm of the loop is represented by the following formulas:

$$x = e_1 d/2\sin\theta \tag{5}$$

$$y = t_1 d/2\cos\theta \tag{6}$$

$$z = a'(S_1)^2 + b'(S_1) + c' \tag{7}$$

where θ is the angle measured from the y″ axis, S1 is the length measured from the y″ axis along the perimeter of the right section of the elliptical cylinder of the yarn arm, and a′, b′, c′ are constants.

The following loop parameters can be derived from the curves that represent the yarn axis of the right arm of the loop:

Distance between axes z and z″ = x_{AC}

$$x_{AC} = \frac{w}{4} = \left(\frac{\chi}{4}\right)d \tag{8}$$

where $\chi = w/d$ and w is the wale spacing.

Horizontal distance between points A and B = x_{AB}.

Thus, we can write

$$x_{AB} = \frac{w}{4} + \frac{e_1 d}{2} = \left(\frac{\chi}{2} + e_1\right)d/2 \tag{9}$$

If the loops are in contact with one another at the wale-jamming point, along the direction of the courses, and there is no yarn compression in the loop interlacing regions, then $e_1=1$.

- **Vassiliadis's model**

The Vassiliadis [26] was employed to create the 3D geometry of the knitted fabric loop. This model represents a three-dimensional structure that closely aligns with the actual shape of the loop in the fabric. In this model, a loop is constructed from four identical segments, with equations applied to describe a quarter of the loop. The geometrical parameters of the loop structure, such as wale spacing, course spacing, and yarn diameter, must be predetermined. Other essential characteristics of the knitted fabric can then be derived from these primary features. Vassiliadis proposed a geometrical construction for a knit loop, where a quarter-loop is composed of three sections: ΣM (from the side view), MK (from the front view), and KA (from the top view). Consequently, a curve equation must be defined for each of these sections. The section ΣM is modeled as an elliptical arc in 3D space. It can be represented as a circular arc with a radius of (r+D/2) in the YZ plane and as a straight line in the XY plane, where D is the diameter of the yarn and r is a derived parameter.

$$r = \left\{ \left(c - \frac{D}{2} - \frac{t}{2} \right)^2 - \left(\frac{D}{2} + \frac{t}{2} \right)^2 \right\} / (2D) \qquad (10)$$

Here, c represents the course spacing, and t is a parameter associated with loop curvature, constrained by the inequality ($0 \leq t \leq c - 2D$). The next section (MK) is also modeled as an elliptic arc in three-dimensional space. It is defined as an arc of the specified circle in the YZ plane and a quarter ellipse with minor and major radii $a=D/(2+h)$ and $b = R$ in the XY plane. The radius R can be calculated using the following equation:

$$R = \frac{c}{2} - \frac{t}{2} - \frac{D}{2} \qquad (11)$$

Thus, the coordinates of the sections ΣM and MK can derive.

C.   CAD Model

The methods used for geometric modeling of knitted fabric structures involved the following steps:

1. Calculation of Yarn Centerline Position: The centerline position of the yarn was calculated based on the geometric model equations described in the previous sections.

2. Input into SolidWorks: The coordinates of points along the central axis of the loop path were entered into SolidWorks software. Using the yarn diameter and loop path, a quarter-loop was drawn in SolidWorks. The cross-section of the yarn was assumed to have a circular shape.

3. Creation of Complete Loop: By utilizing the symmetry tool in SolidWorks, one complete loop was created, leveraging the symmetry of the loop structure.

The schematic structural characteristics of 1×1 rib and interlock knitted fabrics were referenced from Spencer (2001). As shown in Figure 1, a cell containing two courses and two wales was designed. To develop computational fluid dynamics (CFD) modeling, a unit cell from each sample was extracted and input into CFD software. For the rib and interlock structures, the unit cell contained two and four crossovers, respectively. As illustrated in Figure 1, in the rib structure, the location of each knit loop in a wale is the reverse of the lateral loop. In the interlock fabric, there are two rows of knit loops whose positions are opposite in each row. The design of the knitted fabric structure and the fabric unit cells for the 1×1 rib and interlock structures were used for CFD simulation and analysis in the subsequent section.
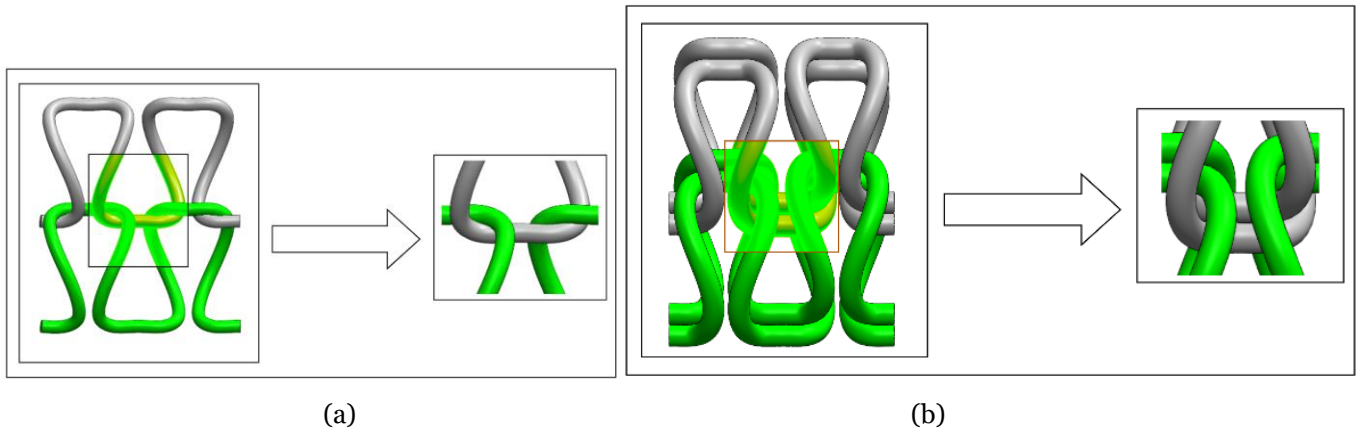
Figure 1: Example of the design of a knitted fabric structure and one fabric unit cell; (a) rib 1×1 and (b) interlock.

D. CFD analysis

A unit cell, representing one segment of the fabric structure, was designed as shown in Fig. 2. For the development of the CFD model, a unit cell from each sample was isolated and input into CFD software. The geometric structure of the loop fabric was simulated with three different set densities in the wale and course directions using SolidWorks software. CFD modeling was then performed using SolidWorks Flow Simulation. The sample was positioned within a pipe-like domain, located 5 mm downstream from the domain inlet and 5 mm upstream from the domain outlet. This setup ensured that airflow was fully developed before interacting with the sample. Incorporating a unit cell in the model significantly reduced computational time due to its smaller dimensions. For the CFD analysis, the k-ε turbulence model, a member of the Eddy Viscosity Models (EVMs), was applied. This model introduces two additional transport equations into the Reynolds-Averaged Navier–Stokes (RANS) equations to account for turbulent kinetic energy (k) and its dissipation rate (ε). In accordance with experimental parameters, the pressure difference across the fabric was set to 100 Pa, as depicted in Fig. 2(a). Figure 2(b) illustrates a computational method for a sample based on the Vassiliadis model, showing air velocity distributions for one unit cell of interlock fabric. The visualization highlights the airflow patterns directly above and below the fabric, along with the shapes of the airflow lines. Due to the model's relatively small dimensions, the use of a unit cell facilitated a reduced computational resolution time without compromising the accuracy of the analysis.
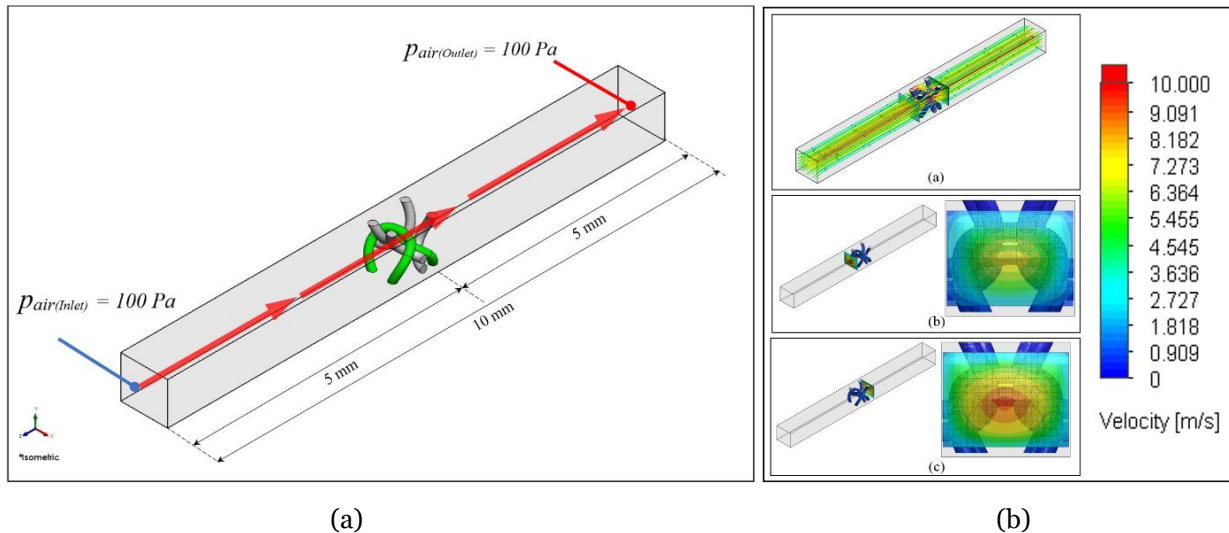
Figure 2: (a) boundary conditions and pressures set; (b) air velocity distributions for one unit cell of interlock fabric positioned directly above, directly below, and visualization of the shape of the air flow lines.

III.   RESULTS AND DISCUSSION

A.   CAD modeling of knitted fabric

The main steps outlined in the previous section provided the foundation for developing our 3D model of knitted fabric structures. The geometrical parameters associated with each knitted fabric loop structure were derived using Peirce's model, Leaf and Glaskin's model, Vassiliadis's model, and Kurbak's model. The parameters used as input for computer-aided modeling were based on the set densities listed in Table 1. The study focused on rib 1x1 structures with wale/cm and course/cm densities of 9/11, 9/13, and 9/14, as well as interlock structures with wale/cm and course/cm densities of 9/11, 11/16, and 11/18. This approach resulted in three different density combinations for each knitted fabric loop structure model. The yarns in both the wale and course directions had identical linear densities and material compositions. The geometric parameters of 24 knitted fabric structures were simulated using SolidWorks software. In the CAD model, the single-line yarn path for each knitted fabric structure was analyzed to predict air permeability.

Figure 3 illustrates the top views of knitted fabric structures (1×1 cm²) for three different set densities of rib 1×1 and interlock fabric. A total of 24 samples, encompassing four geometrical models of weft-knitted fabrics and three set densities, were analyzed. The wale and course densities were found to significantly influence the shapes and sizes of the pores. Increased wale and course densities within the 1×1 cm² area resulted in reduced pore sizes, altering their shapes and hydraulic diameters. Higher wale and course densities tended to produce pores that were more square-like, with larger hydraulic diameters, thereby facilitating greater air permeability. Figure 4 depicts a single-unit cell fabric structure designed using SolidWorks software. This model, represented by a single line, was utilized for CFD simulation analysis in the subsequent section. Based on the CAD models in Figures 3 and 4, an increase in the set density in the wale and course directions of the knitted fabric corresponded to a decrease in the porosity of the fabric structure.

B.   CFD Modeling of knitted fabric

Based on the boundary conditions for airflow simulations described in the previous section, air permeability was simulated using single-line yarn path models. An example of the simulation results for air velocity distributions in one unit cell of interlock fabric positioned directly above and below along with a visualization of the airflow lines, is shown in Figure 2 (a, b). The following formula is then used to compute the value of air permeability (R).

$$R = Q / A_t \tag{12}$$
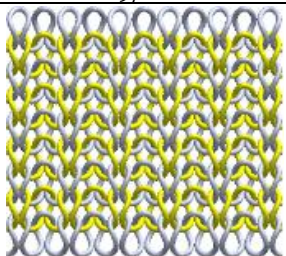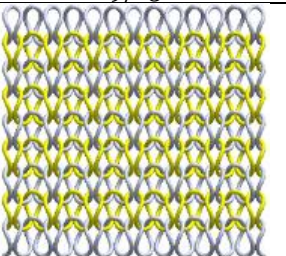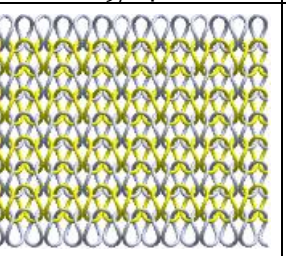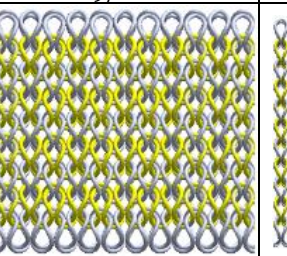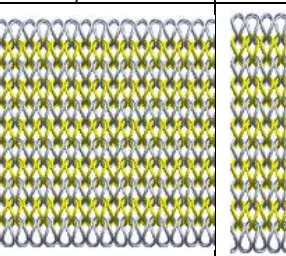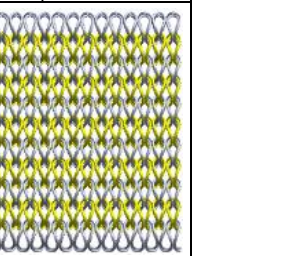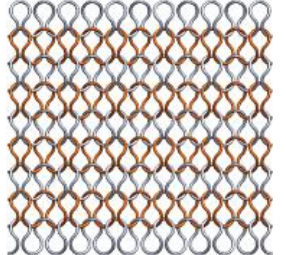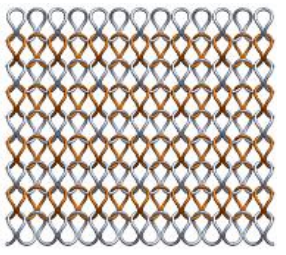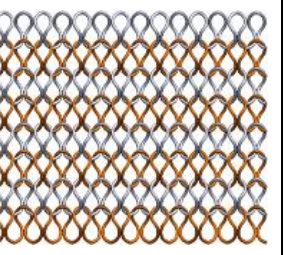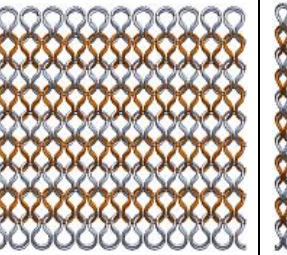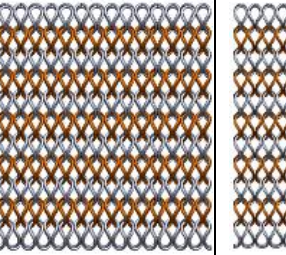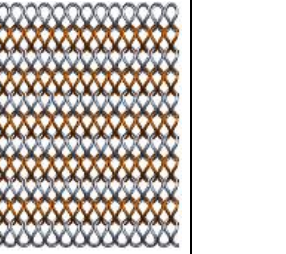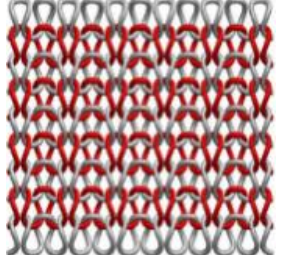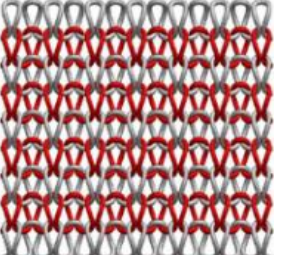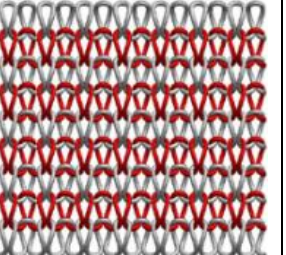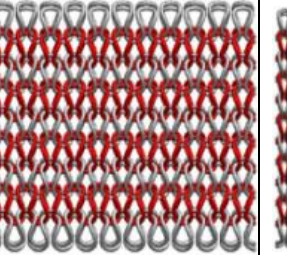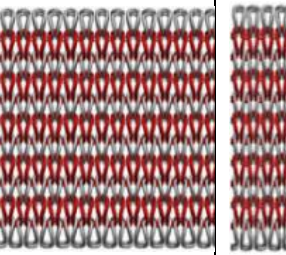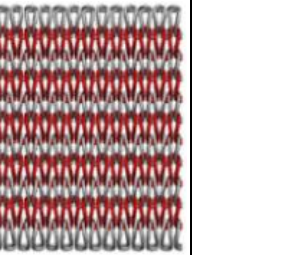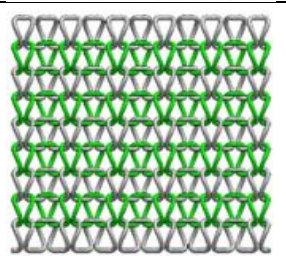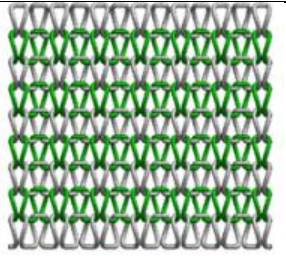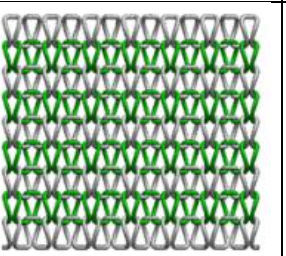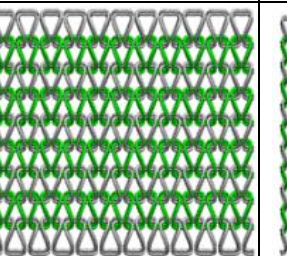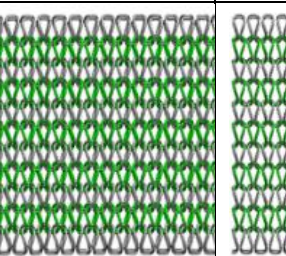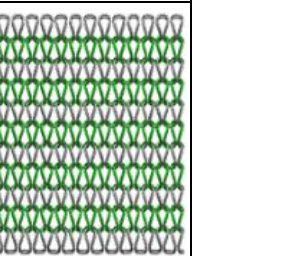
Model	Rib 1x1 (Wale/Course)			interlock (Wale/Course)		
	9/11	9/13	9/14	9/11	11/16	11/18
Peirce models						
Leaf and Glaskin models						
Kurbak models						
Vassilidis models						

Figure 3: CAD model (Top view) of 1x1 cm² of rib (1x1) and interlock surfaces of fabric samples.

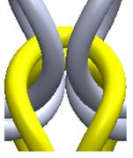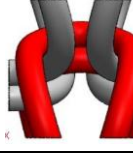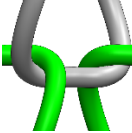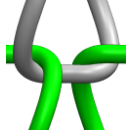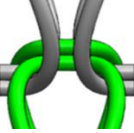| Model	Rib 1x1 (Wale/Course)			Interlock (Wale/Course)		
	9/11	9/13	9/14	9/11	11/16	11/18
Peirce models						
Leaf and Glaskin models						
Kurbak models						
Vassilidis models						

Figure 4: Fabric structure designed of yarn path for rib 1x1 and interlock in 1 unit cell (Peirce models, Leaf and Glaskin models, Kurbak models and Vassilidis models).

The cloth area under test is denoted as A_t. The air flow rate for the fabric (Q) is measured using an air permeability tester. Air permeability refers to the velocity of air passing through the fabric. Figure 5 illustrates the velocity field simulation results for all sample models, showing the air flow moving from the inlet to the outlet due to the pressure difference between the two sides of the sample. As the air flow interacts with the knitted fabric, it deviates toward the pore locations to pass through the material.

This interaction increases the air flow velocity. After passing through the fabric, the air flow resumes its direct path. Figures 5(a–d) provide a detailed depiction of this phenomenon. A decrease in the sample's pore size, caused by an increase in loop density, results in reduced air permeability. The prediction results for the four knitted fabric models, along with the experimental air permeability results and percentage errors, are summarized in Table 2. Additionally, Figure 6 compares the air permeability simulation results for different knitted fabric models with the corresponding experimental data. Among the four simulation models, the Kurbak model demonstrated the lowest error, followed by the Peirce model, the Leaf and Glaskin model, and the Vassiliadis model, respectively. Notably, the results of all four simulation models were higher than the experimental results, but there is strong agreement between the predicted and experimental data. Using the actual structural parameters of rib 1x1 and interlock knitted fabrics, with specific wale and course densities, results in a more accurate simulation geometry. Therefore, computational fluid dynamics (CFD) can be applied in predicting fabric air permeability.

Increasing the loop density reduces the pore size within the sample, thereby decreasing air permeability. Moreover, due to the presence of two layers of structural interlock compared to the rib structure, samples with an interlock structure exhibit lower air permeability than those with a rib structure (e.g., sample R-1 compared to sample I-1). The existence of two rows in interlock fabric further decreases porosity in these fabric structures. In particular, the overlap of loops is a significant factor contributing to the reduction in fabric porosity in interlock structures. A comparison between the numerical and experimental results is presented in Table 2.

The study by Unal [27] demonstrates a substantial negative correlation between yarn hairiness and the air permeability of single jersey fabric. Specifically, an increase in yarn hairiness results in reduced air permeability and greater friction between the fibers and airflow. In this study, yarn was assumed to have no hairiness, which may partly explain the discrepancy between experimental and numerical results. It is important to note that in real

textile materials, the strength of individual yarn section fastenings within knitted fabric and the associated pressure drop can influence how airflow alters the hole shape. These complexities present significant challenges when attempting to integrate them into physical process models and existing geometric models of knitted structures.

Airflow in real fabric structures can also alter pore geometry, influenced by the pressure drop and the strength of the fastening of individual yarn sections within the fabric structure [28]. Addressing these dynamic changes remains a significant challenge in current geometric and physical models, thereby limiting the accuracy of simulation results. Denting, a critical technological parameter, plays a substantial role in determining air permeability. Variations in the distances between wale and course yarns due to denting lead to differences in pore size, distribution, and shape. Future research should focus on incorporating the effects of denting to improve the predictive accuracy of air permeability models.
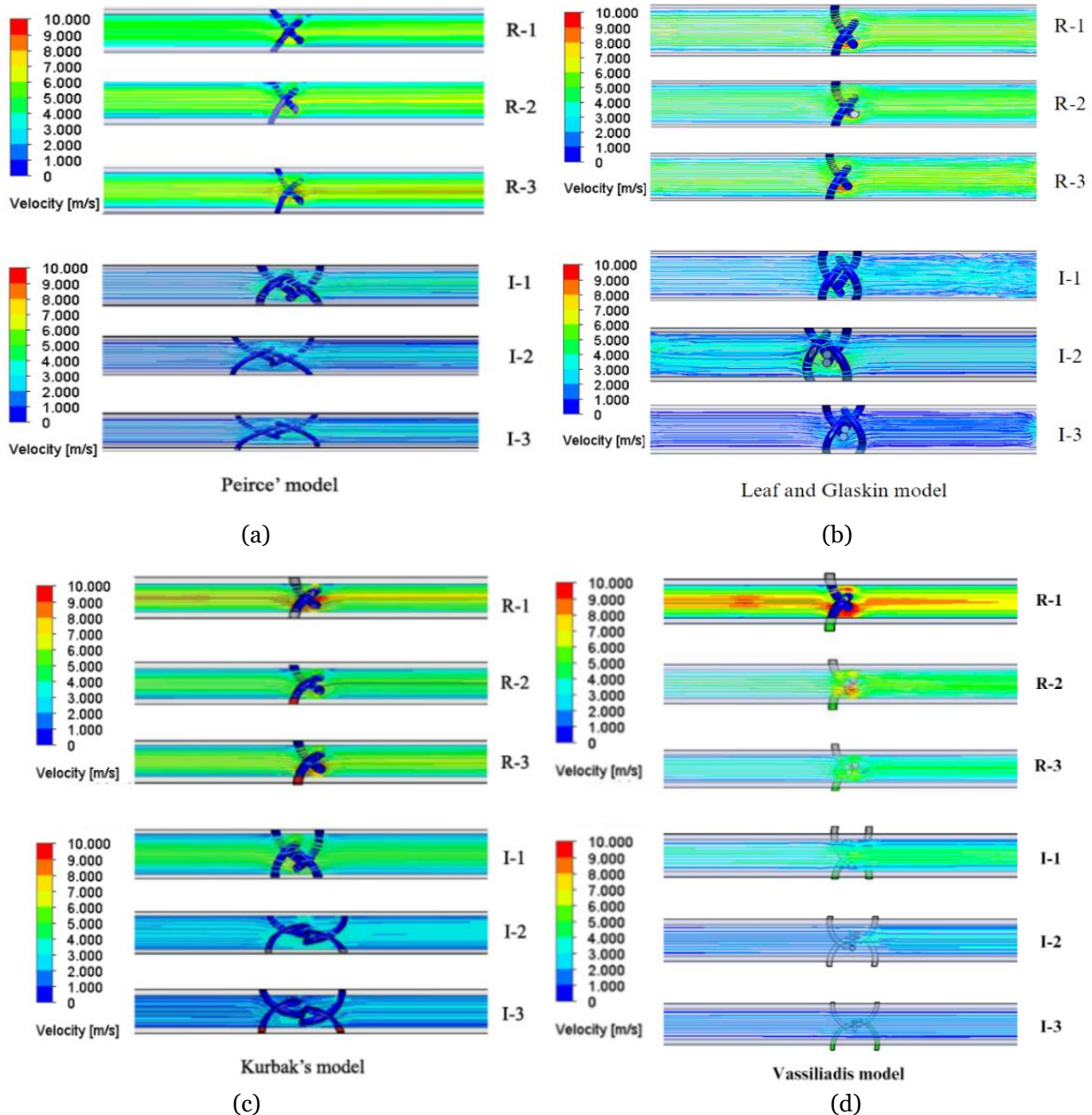

Figure 5: Velocity counters for all samples; (a) Peirce models, (b) Leaf and Glaskin models, (c) Kurbak models and (d) Vassilidis models.

Table 2: Prediction model, experimental air permeability results and % error.

| Simple code	Experimental air permeability results ($ml/s. cm2$)	Prediction air permeability results (m^3/s)				Error of air permeability results (%)			
		Peirce model	Leaf and Glaskin model	Kurbak model	Vassiliadis model	Peirce model	Leaf and Glaskin model	Kurbak model	Vassiliadis model
R-1	364	404.8	424.9	412.2	413.4	11.2	16.7	13.2	13.6
R-2	321	359.5	374.5	353.2	379.2	11.9	16.6	10.1	18.1
R-3	290	325.6	335	321.1	340.9	12.2	15.5	10.7	17.6
I-1	275	317.4	308.4	312.3	309.1	15.4	12.1	13.5	12.4
I-2	156	180.7	177.7	171.4	184.0	15.8	13.9	9.8	17.9
I-3	140	156.9	159.8	156.7	158.8	12.1	14.1	11.9	13.4
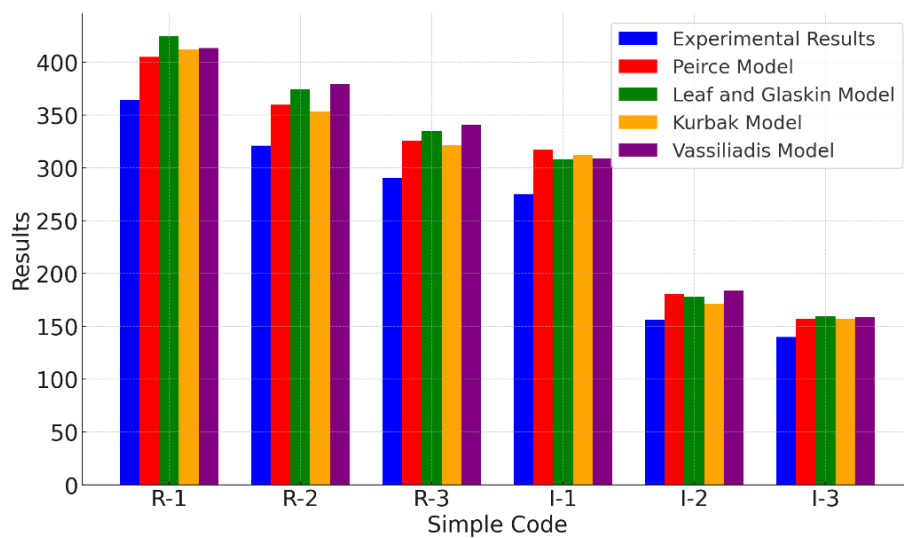
Figure 6: Comparison of air permeability simulation results for different knitted fabric model with experimental data.

IV. CONCLUSION

The air permeability test for rib 1x1 and interlock-pattern knitted fabric structures was simulated using the CFD technique. Among the four simulation models analyzed, the Kurbak model exhibited the lowest error value, followed by the Peirce model, the Leaf and Glaskin model, and the Vassiliadis model, respectively. However, the results from all four simulation models were higher than the experimental results, indicating good agreement between the predicted and experimental values. The error percentages ranged between 9.80% and 18.10%. An increased set density in the wale and course directions of knitted fabric led to decreased air permeability. At the same loop density, knitted fabrics with an interlock structure demonstrated lower air permeability compared to those with a rib structure. Furthermore, the CFD method was verified and successfully applied for predicting and investigating the air permeability of rib 1x1 and interlock-pattern knitted fabric structures. By utilizing unit cells of knitted fabric created using 3D geometry, the computational solving time was reduced, while the accuracy of the CFD results was improved. A more precise geometric model of knitted fabrics could be incorporated into the simulation for further development.

REFERENCES

[1]   Ettehadi, Z.; Ajeli, S.; Soltani, P.; and Zarrebini, M. Experimental and CFD Analysis of Air Permeability of Warp-knitted Structures. Fibers and Polymers. 2020, 21, 1362-1371.

[2]   Burleigh, E.G.; Wakeham, H.J.R, et al. Pore-size distribution in textiles. Textil Res J. 1949, 19, 547–555.

[3] Ogulata R.T.; Mavruz, S. Investigation of Porosity and Air Permeability Values of Plain Knitted Fabrics. Fibres and Textiles in Eastern Europe. 2010, 18, 71–75.

[4] Arumugam, V.; Mishra, R.; Militky, J.; Salacova, J. Investigation on thermo-physiological and compression characteristics of weft-knitted 3D spacer fabrics. Journal of The Textile Institute. 2017, 108, 1095-1105.

[5] Ghada, A.M. Comparative Study of Air Permeability of Polyester/Metallic Blended Woven Fabrics. Life Science Journal. 2015, 12, 78–82.

[6] Zupin, Z.; Hladnik, A. Dimitrovski. Prediction of one-layer woven fabrics air permeability using porosity parameters. Textile Research Journal. 2011, 82, 117–128.

[7] Polipowski, M.; Więcek,P.; Więcek,B.; Jasińska, I. Study on Woven Fabric Structure Using 3D Computer Image Analysis for In-Depth Identification of Thread Channels. Fibres and Textiles in Eastern Europe. 2015 23, 33–39.

[8] Kyosev, Y.; Angelova, Y.; Kovar, R. 3D modeling of plain weft knitted structures of compressible yarn. Res J Text Appar. 2005, 9, 88–97.

[9] Kaldor, J.M.; James, D.L.; Marschner, S. Simulating knitted cloth at the yarn level. ACM T Graphic. 2008, 65, 1-9.

[10] Wadekar, P.; Goel, P.; Amanatides, C.; Dion, G.; Kamien, R.D.; Breen, D.E. Geometric modeling of knitted fabrics using helicoid scaffolds. J. Eng. Fibers Fabr. 2020, 15, 1–15.

[11] Sriprateep, K.; Pattiya, A. Computer aided geometric modeling of twist fiber. Journal of Computer Science. 2009. 5. 221-226.

[12] Sriprateep, K.; Singto, S. New computer geometric modeling approach with filament assembly model for two-ply yarns structures The Journal of the Textile Institute. 2019, 110, 1307-1317.

[13] Patumchat, P.; Sriprateep, K. New computer geometric modeling approach with filament assembly model for woven fabric structures. The Journal of the Textile Institute. 2019, 110, 50-60.

[14] Patumchat, P.; Sriprateep, K. Computer geometric modeling approach with filament assembly model for 2× 2 twill woven fabrics structures. Indian Journal of Fibre & Textile Research. 2023, 48, 132-140.

[15] Patumchat, P.; Inthidech, S.; Srithep, Y.; Sriprateep K. Computer geometric modeling approach with filament assembly model for 2×1 and 3×1 twill woven fabric structures. Autex Research Journal. 2023, 23, 522-531.

[16] Sriprateep, K.; Bohez, E.L.J. CAD/CAE for stress–strain properties of multifilament twisted yarns. Textile Research Journal. 2017, 87, 657–668.

[17] Sriprateep, K. CAD/CAE for stress–strain properties of a wide range of multifilament twisted man-made filament yarns. Textile Research Journal. 2019, 89, 204-215.

[18] Puszkarz, A.; Krucinska, I. Modelling of air permeability of knitted fabric using the computational fluid dynamics. AUTEX Res. J. 2018, 18, 364–376.

[19] Puszkarz, A.; Krucinska, I. The study of knitted fabric thermal insulation using thermography and finite volume method. Text. Res. J. 2017, 87, 643–656.

[20] Cimilli, S. D.; Deniz, E.; Candan, C.; Nergis, B. Determination of Natural Convective Heat Transfer Coefficient for Plain Knitted Fabric via CFD Modeling. Fibres&Text. Eas. Euro. 2012, 90, 42-46.

[21] Dehkordi, H.; Ghane, M.; Abdellahi, S.B.; Soultanzadeh, B. Numerical Modeling of the Air Permeability of Knitted Fabric Using Computational Fluid Dynamics Method. Fibers and Polymers. 2017, 18, 1804-1809.

[22] Peirce, F.T. Geometrical Principles Applicable to the Design of Functional Fabrics. Textil. Res. J. 1947, 17 123–147.

[23] Leaf, G.A.V.; Glaskin, A. Geometry of Plain-Knitted Loop, J. Textil. Inst. 1955, 46, 587–605.

[24] Kurbak, A. Plain Knitted Fabric Dimensions (Part II). Textile Asia, 1998, 29, 36-44.

[25] Kurbak, A.; Ekmen, O. Basic Studies for Modeling Complex Weft Knitted Fabric Structures Part I: A Geometrical Model for Widthwise Curlings of Plain Knitted Fabrics. Textile Research Journal. 2008, 78, 198–208.

[26] Vassiliadis, S.G.; Kallivretaki, A.E.; Provatidis, C.G. Geometrical Modelling of Plain Weft Knitted Fabrics, Indi. J. Fib. Text. Res. 2007, 32, 62-71.

[27] Unal, P.G.; Üreyen, M. E.; Mecit D. Predicting properties of single jersey fabrics using regression and artificial neural network models. Fibers and Polymers. 2012, 13, 87-95.

[28]   Ielina, T.; Halavska, L.; Mikucioniene, D.; Milasius, R.; Bobrova, S.; Dmytryk, O. Development of 3D
        Models of Knits from Multi-Filament Ultra-Strong Yarns for Theoretical Modelling of Air Permeability.
        Materials. 2021, 14, 3489.